Investigation of $cs\bar{c}\,\bar{s}$ tetraquark in the chiral quark model

Yifan Yang and Jialun Ping*

Department of Physics and Jiangsu Key Laboratory for Numerical Simulation of Large Scale Complex Systems, Nanjing Normal University, Nanjing 210023, People's Republic of China

(Received 1 April 2019; published 23 May 2019)

Inspired by the recent observation of exotic resonances $X(4140)$, $X(4274)$, $X(4350)$, $X(4500)$, and $X(4700)$ reported by several experiment collaborations, we investigated the four-quark system $cs\bar{c}\,\bar{s}$ with quantum numbers $J^{PC} = 1^{++}$ and 0^{++} in the framework of the chiral quark model. Two configurations, diquark-antidiquark and meson-meson, with all possible color structures are considered. The results show that no molecular state can be formed, but the resonance may exist if the color structure of the meson-meson configuration is $8 \otimes 8$. In the present calculation, the $X(4274)$ can be assigned as the $cs\bar{c}\,\bar{s}$ tetraquark states with $J^{PC} = 1^{++}$, but the energy of $X(4140)$ is too low to be regarded as the tetraquark state. $X(4350)$ can be a good candidate of the compact tetraquark state with $J^{PC} = 0^{++}$. When the radial excitation is taken into account, the $X(4700)$ can be explained as the $2S$ radial excited tetraquark state with $J^{PC} = 0^{++}$. As for $X(4500)$, there is no matching state in our calculation.

DOI: 10.1103/PhysRevD.99.094032

I. INTRODUCTION

Recently, several exotic resonances were observed in the invariant mass distribution of $J/\psi\phi$. In 2009, the CDF Collaboration found the $X(4140)$ with mass $M = 4143.0 \pm 2.9 \pm 1.2$ MeV and width $\Gamma = 11.7^{+8.4}_{-6.7} \pm 3.7$ MeV in $B^+ \to J/\psi\phi K^+$ decay [1]. In 2010, a narrow resonance $X(4350)$ with mass $M = 4350.6^{+4.6}_{-5.1} \pm 0.7$ MeV and width $\Gamma = 13^{+18}_{-9} \pm 4$ MeV was reported by the Belle Collaboration in the $\gamma\gamma \to J/\psi\phi$ process, and the possible spin parity is $J^{PC} = 0^{++}$ or 2^{++} [2]. A few years later, the exotic resonance $X(4140)$ was observed by some other collaborations including LHCb, D0, CMS, and *BABAR* [3–6]. In 2011, another resonance $X(4274)$ with mass $M = 4274.4 \pm 1.9$ MeV and width $\Gamma = 32.3 \pm 7.6$ MeV was observed by the CDF Collaboration in $B^+ \to J/\psi\phi K^+$ decay with 3.1σ significance [7]. In 2016, the LHCb Collaboration performed the first full amplitude analysis of the $B^+ \to J/\psi\phi K^+$ process, and the existence of the $X(4140)$ and $X(4274)$ was confirmed. Their quantum numbers are fixed to be $J^{PC} = 1^{++}$ [8]. At the same time, the collaboration observed two other resonances, $X(4500)$ and $X(4700)$, with $J^{PC} = 0^{++}$. Their masses and decay widths have been determined as [9]

$$M_{X(4500)} = (4506 \pm 11^{+12}_{-15})\ \text{MeV}, \tag{1}$$

$$\Gamma_{X(4500)} = (92 \pm 21^{+21}_{-20})\ \text{MeV}, \tag{2}$$

$$M_{X(4700)} = (4704 \pm 10^{+14}_{-24})\ \text{MeV}, \tag{3}$$

$$\Gamma_{X(4500)} = (120 \pm 31^{+42}_{-33})\ \text{MeV}. \tag{4}$$

With the discovery of these exotic resonances, many theoretical works, such as approaches based on quark models [10–14], QCD sum rules [15], etc., have been performed. In the framework of the relativized quark model, the $X(4140)$ can be regarded as the $cs\bar{c}\,\bar{s}$ tetraquark ground state, and the $X(4700)$ can be explained as the $2S$ excited tetraquark state [10]. Based on the simple color-magnetic interaction model, possible ground $cs\bar{c}\,\bar{s}$ tetraquark states in the diquark-antidiquark configuration have been investigated, and the interpretation of $X(4500)$ and $X(4700)$ needs orbital (radial or angular) excitation [11]. Deng *et al.* investigated the hidden charmed states in the framework of the color flux-tube model, and they found that the energy of the first radial excited state $(cs)(\bar{c}\,\bar{s})$ with 2^5D_0 is in full accord with that of the state $X(4700)$ [12]. In a simple quark model with chromomagnetic interaction, Stancu suggested that the $X(4140)$ could possibly be the strange partner of $X(3872)$ in a tetraquark interpretation [13]. Lebed and Polosa argued that $X(4140)$ was a $J^{PC} = 1^{++}$ $c\bar{c}s\bar{s}$ state in the diquark-antidiquark model because it has been not been seen in two-photon fusion [16]. Ortega *et al.* claimed that the $X(4140)$ resonance appeared as a cusp in the $J/\psi\phi$ channel due to the near coincidence of the

*jlping@njnu.edu.cn

$D_s^\pm D_s^{*\pm}$ and $J/\psi\phi$ mass thresholds when the nonrelativistic constituent quark model was employed [14]. According to the QCD sum rules, Chen *et al.* pointed out that the $X(4500)$ and $X(4700)$ may be interpreted as the D-wave $cs\bar{c}\,\bar{s}$ tetraquark states with opposite color structures [15]. Recently, an approach, which tried to unify the description of "XYZ" particles, based on the Born-Oppenheimer approximation, was applied to the tetraquark system with double heavy flavors [17,18], $X(4140)$, $X(4274)$, and $X(4350)$, all taken as $c\bar{c}s\bar{s}$ tetraquarks [17]. It should be emphasized that most of these explanations do not agree with each other, and many of these investigations neglected the spin-orbital interaction when the orbital excitations were taken into account.

To see whether these exotic resonances can be described by $cs\bar{c}\,\bar{s}$ tetraquark systems with $J^{PC} = 0^{++}, 1^{++}$, we do a high-precision four-body calculation based on the framework of the chiral quark model, which describes the hadron spectra and hadron-hadron interaction well [19,20]. The high-precision few-body method, the Gaussian expansion method (GEM) [21], is employed for this purpose. Two configurations, $(q\bar{q})(q\bar{q})$ (meson-meson) and $(qq)(\bar{q}\,\bar{q})$ (diquark-antidiquark), are considered. All the color constructions for each configuration are taken into account. For the meson-meson configuration, the color structures are $1 \otimes 1$ and $8 \otimes 8$, and for the diquark-antidiquark configuration, the color structures are $\bar{3} \otimes 3$ and $6 \otimes \bar{6}$. To explain the two higher exotic resonances $X(4500)$ and $X(4700)$, the orbital excitation with the inclusion of spin-orbital interaction is invoked. To expose the structures of the states, the distances between two quarks (antiquarks) for given states are calculated.

This paper is organized as follows. In Sec. II, the chiral quark model and wave functions of $cs\bar{c}\,\bar{s}$ tetraquark systems are introduced. The numerical results and a discussion are presented in Sec. III. Finally, we give a brief summary of our investigation and the future work to be done in Sec. IV.

II. CHIRAL QUARK MODEL AND WAVE FUNCTIONS

The chiral quark model has achieved great success when describing hadron spectra and hadron-hadron interactions [20]. The specific introduction of the chiral quark model can be found in Ref. [19]. The Hamiltonian of $cs\bar{c}\,\bar{s}$ tetraquark systems, which is shown below, includes the mass, the kinetic energy, and different kinds of interactions. These interactions include the confinement V^C, one-gluon-exchange V^G, and Goldstone bosons exchanges $V^\chi(\chi = \pi, \kappa, \eta)$; only η exchange plays a role between s and $\bar{s}$. Scalar meson exchange V^σ is not included in these interactions because it is expected to exist between $u(\bar{u})$ and $d(\bar{d})$ only. Because of the existence of orbital excitation, the spin-orbit coupling terms are also taken into consideration,

$$H = \sum_{i=1}^{4}\left(m_i + \frac{p_i^2}{2m_i}\right) - T_{cm} + \sum_{i=1<j}^{4}\left(V_{ij}^C + V_{ij}^G + \sum_{\chi=\pi,\kappa,\eta} V_{ij}^\chi\right) + V_{Q\bar{Q}}^{C,LS} + V_{Q\bar{Q}}^{G,LS}, \quad (5)$$

$$V_{ij}^C = (-a_c r_{ij}^2 - \Delta)\boldsymbol{\lambda}_i^c \cdot \boldsymbol{\lambda}_j^c \quad (6)$$

$$V_{ij}^G = \frac{\alpha_s}{4}\boldsymbol{\lambda}_i^c \cdot \boldsymbol{\lambda}_j^c\left[\frac{1}{r_{ij}} - \frac{2\pi}{3m_i m_j}\boldsymbol{\sigma}_i \cdot \boldsymbol{\sigma}_j \delta(\boldsymbol{r}_{ij})\right], \quad (7)$$

$$V_{ij}^\pi = \frac{g_{ch}^2}{4\pi}\frac{m_\pi^2}{12m_i m_j}\frac{\Lambda_\pi^2 m_\pi}{\Lambda_\pi^2 - m_\pi^2}\boldsymbol{\sigma}_i \cdot \boldsymbol{\sigma}_j\left[Y(m_\pi r_{ij}) - \frac{\Lambda_\pi^3}{m_\pi^3}Y(\Lambda_\pi r_{ij})\right] \times \sum_{a=1}^{3}\boldsymbol{\lambda}_i^a \cdot \boldsymbol{\lambda}_j^a, \quad (8)$$

$$V_{ij}^\kappa = \frac{g_{ch}^2}{4\pi}\frac{m_\kappa^2}{12m_i m_j}\frac{\Lambda_\kappa^2 m_\kappa}{\Lambda_\kappa^2 - m_\kappa^2}\boldsymbol{\sigma}_i \cdot \boldsymbol{\sigma}_j\left[Y(m_\kappa r_{ij}) - \frac{\Lambda_\kappa^3}{m_\kappa^3}Y(\Lambda_\kappa r_{ij})\right] \times \sum_{a=4}^{7}\boldsymbol{\lambda}_i^a \cdot \boldsymbol{\lambda}_j^a, \quad (9)$$

$$V_{ij}^\eta = \frac{g_{ch}^2}{4\pi}\frac{m_\eta^2}{12m_i m_j}\frac{\Lambda_\eta^2}{\Lambda_\eta^2 - m_\eta^2}m_\eta \boldsymbol{\sigma}_i \cdot \boldsymbol{\sigma}_j\left[Y(m_\eta r_{ij}) - \frac{\Lambda_\eta^3}{m_\eta^3}Y(\Lambda_\eta r_{ij})\right] \times [\cos\theta_P(\boldsymbol{\lambda}_i^8 \cdot \boldsymbol{\lambda}_j^8) - \sin\theta_P(\boldsymbol{\lambda}_i^0 \cdot \boldsymbol{\lambda}_j^0)], \quad (10)$$

where T_{cm} is the kinetic energy of the center-of-mass motion; $Y(x)$ is the standard Yukawa functions; the $\boldsymbol{\sigma}$ and $\boldsymbol{\lambda}$ represent Pauli and Gell-Mann matrices, respectively; and the strong coupling constant of one-gluon exchange is α_s, the running property of which is given as

$$\alpha_s(\mu_{ij}) = \frac{\alpha_0}{\ln[(\mu_{ij}^2 + \mu_0^2)/\Lambda_0^2]}, \quad (11)$$

where μ_{ij} represents the reduced mass of two interacting particles.

For the diquark-antidiquark configuration, the subclusters qq and $\bar{q}\,\bar{q}$ can be treated as compound bosons $\bar{Q}$ and Q with no internal orbital excitation. If the relative orbital angular excitations between the two clusters is $\boldsymbol{L}$, the four-body spin-orbit interactions can be simply expressed as [22,23]

$$V_{Q\bar{Q}}^{C,LS} = -a_c \boldsymbol{\lambda}_Q^c \cdot \boldsymbol{\lambda}_{\bar{Q}}^c \frac{1}{4M_Q M_{\bar{Q}}}\boldsymbol{L} \cdot \boldsymbol{S} \quad (12)$$

$$V_{Q\bar{Q}}^{G,LS} = -\frac{\alpha_s}{4}\boldsymbol{\lambda}_Q^c \cdot \boldsymbol{\lambda}_{\bar{Q}}^c \frac{1}{8M_Q M_{\bar{Q}}}\frac{3}{X^3}\boldsymbol{L} \cdot \boldsymbol{S}, \quad (13)$$

where the $M_Q(M_{\bar{Q}})$ is the total mass of subcluster, $\boldsymbol{X}$ is the distance between the two clusters, and $\boldsymbol{S}$ is the total spin of the tetraquark state. This simplification can be generalized

TABLE I. Parameters of the chiral quark model.

Parameters	Values	Parameters	Values
m_u (MeV)	313	$\Lambda_\pi = \Lambda_\sigma$ (fm^{-1})	4.2
m_d (MeV)	313	$\Lambda_\eta = \Lambda_\kappa$ (fm^{-1})	5.2
m_s (MeV)	536	$g_{ch}^2/(4\pi)$	0.54
m_c (MeV)	1728	$\theta_p(°)$	−15
m_b (MeV)	5112	a_c (MeV)	101
m_π (fm^{-1})	0.70	Δ (MeV)	−78.3
m_σ (fm^{-1})	3.42	α_0	3.67
m_η (fm^{-1})	2.77	Λ_0 (fm^{-1})	0.033
m_κ (fm^{-1})	2.51	μ_0 (MeV)	36.976

to color-octet meson subclusters in the meson-meson configuration.

In this paper, the model parameters of the chiral quark model are directly taken from our previous work [24], which is shown in Table I. These parameters are obtained by fitting the meson spectrum. Some of the calculated meson spectra have been given in Table II.

Next, we will introduce the wave functions for the $cs\bar{c}\,\bar{s}$ tetraquark. A quark (antiquark) has 4 degrees of freedom, including orbit, flavor, spin, and color. For each degree of freedom, first we construct the wave function for each subcluster and then couple the wave functions of two subclusters to get the wave functions for the final tetraquark systems.

For the spatial part, the total spatial wave functions of tetraquark systems can be obtained by coupling three relative orbital motion wave functions,

$$\psi_{LM_L} = [[\psi_{l_1}(\mathbf{r}_{12})\psi_{l_2}(\mathbf{r}_{34})]_{l_{12}}\psi_{L_r}(\mathbf{R})]_{LM_L}, \tag{14}$$

where $\psi_{l_1}(\mathbf{r}_{12})$ and $\psi_{l_1}(\mathbf{r}_{34})$ are the relative orbital motions between two particles in each subcluster with angular momentum l_1 and l_2, respectively, and $\psi_{L_r}(\mathbf{R})$ is the relative orbital wave function between two subclusters with angular momentum L_r. In the present calculation, we do not consider the orbital excitation in each subcluster, so we set $l_1 = l_2 = 0$ and $L_r = L$, which is the total orbital angular momentum of tetraquark systems. In GEM, three relative orbital motion wave functions are all expanded by Gaussian functions [21],

$$\psi_{lm}(\mathbf{r}) = \sum_{n=1}^{n_{\max}} c_{nl}\phi^G_{nlm}(\mathbf{r}) \tag{15}$$

$$\phi^G_{nlm}(\mathbf{r}) = N_{nl} r^l e^{-\nu_n r^2} Y_{lm}(\hat{\mathbf{r}}) \tag{16}$$

$$N_{nl} = \left(\frac{2^{l+2}(2\nu_n)^{l+3/2}}{\sqrt{\pi}(2l+1)!!}\right)^{\frac{1}{2}}, \tag{17}$$

where N_{nl} are normalization constants, and the expansion coefficients c_{nl} are obtained by solving the Schrödinger equation. The Gaussian size parameters are set according to the geometric progression

$$\nu_n = \frac{1}{r_n^2}, \quad r_n = r_{\min} a^{n-1}, \quad a = \left(\frac{r_{\max}}{r_{\min}}\right)^{\frac{1}{n_{\max}-1}}, \tag{18}$$

where the $n_{\max}$ is the number of Gaussian functions and a is the ratio coefficient. After parameter optimization through continuous calculation, we find the calculation results begin to converge, when $n_{\max} = 7$.

For the spin part, since the spin of each quark (antiquark) is $1/2$, the spin of each subcluster can only be 0 or 1. After coupling the spins of the two subclusters, the total spin of tetraquark may be 0, 1, and 2. The total spin S of the tetraquark system is obtained from the coupling $S_1 \otimes S_2 \to S$, where S_1 and S_2 represent the spins of two subclusters. We use $\chi_i (i = 1 \sim 6)$ to denote the total spin wave functions of tetraquark systems. All of the six possible spin channels are given as

$$\begin{aligned} &\chi_1\colon\ 0\otimes 0 \to 0 \quad \chi_2\colon\ 1\otimes 1\to 0\\ &\chi_3\colon\ 0\otimes 1\to 1 \quad \chi_4\colon\ 1\otimes 0\to 1 \quad \chi_5\colon\ 1\otimes 1\to 1\\ &\chi_6\colon\ 1\otimes 1\to 2. \end{aligned} \tag{19}$$

For the flavor part, the isospins of all quarks (antiquarks) are all zero, so there is no need to consider the coupling of the isospin. We use $\varphi_j (j = 1 \sim 3)$ to represent the total flavor wave functions of tetraquark systems, and they can be written as

$$\begin{aligned} \varphi_1 &= (c\bar{c})(s\bar{s}),\\ \varphi_2 &= (c\bar{s})(s\bar{c}),\\ \varphi_3 &= (cs)(\bar{c}\,\bar{s}), \end{aligned} \tag{20}$$

where φ_1 and φ_2 are for the meson-meson configuration and φ_3 is for the diquark-antidiquark configuration.

For the color part, there are four different color wave functions of tetraquark systems, which are denoted by $\omega_k (k = 1 \sim 4)$. ω_1 and ω_2 stand for the color singlet-singlet $1 \otimes 1$ and octet-octet $8 \otimes 8$ in the meson-meson configuration, respectively. The remaining two color wave functions ω_3 and ω_4 stand for the color antitriplet-triplet $\bar{3} \otimes 3$

TABLE II. Meson spectra (in mega-electron-volts).

Mesons	E	PDG [25]	Mesons	E	PDG [25]
π	140.1	139.6	D_s	1953.4	1968.3
ρ	774.4	775.3	D_s^*	2080.2	2112.2
ω	708.2	782.7	ϕ	1015.8	1019.5
K	496.4	493.7	η'	824.0	957.8
K^*	918.4	891.8	η_c	2986.3	2983.9
D	1875.4	1869.7	J/ψ	3096.4	3096.9
D^*	1986.3	2010.3			

and sextet-antisextet $6 \otimes \bar{6}$ in the diquark-antidiquark configuration, respectively. The specific construction process and forms of these color wave functions can be found in Ref. [24].

Finally, the total wave functions for the tetraquark systems can be given as

$$\Psi^{ijk}_{LJM_J} = \mathcal{A}[\psi_L \chi_i]^J_{M_J} \varphi_j \omega_k,$$
$$(i = 1 \sim 6, j = 1 \sim 3, k = 1 \sim 4), \quad (21)$$

where J is the total angular momentum and M_J is the third component of the total angular momentum. Because of the two quarks (antiquarks) in $cs\bar{c}\,\bar{s}$, tetraquark systems are all nonidentical particles, the antisymmetrization operator $\mathcal{A} = 1$.

The eigenenergies of the tetraquark systems can be obtained by solving the Schrödinger equation

$$H\Psi^{ijk}_{LJM_J} = E^{ijk}_{LJM_J} \Psi^{ijk}_{LJM_J}, \quad (22)$$

where the Hamiltonian H and wave functions $\Psi^{ijk}_{LJM_J}$ have been given in Eqs. (5) and (21), respectively.

III. NUMERICAL RESULTS AND DISCUSSIONS

The J^{PC} of these exotic resonances observed recently in $B^+ \to J/\psi\phi K^+$ decay are fixed to 1^{++} and 0^{++}. In our current calculation, only the states with these two sets of quantum numbers are considered. Because the parities of these exotic resonances is positive, the total orbital angular momentum L must be even, so must L_r, according to Eq. (14). Meanwhile, these exotic resonances all have the definite positive C parity, and we need to combine the spin and flavor wave functions to construct the eigenstates of the charge conjugate operator. We use $[(q\bar{q})^{S_1}(q\bar{q})^{S_2}]^S$ and $[(qq)^{S_1}(\bar{q}\,\bar{q})^{S_2}]^S$ to represent the combination of spin and flavor wave functions. According to Ref. [26], all of these eigenstates with positive C parity are given as

$$\chi_5\varphi_1 = [(c\bar{c})^1(s\bar{s})^1]^1, \quad (23)$$

$$\chi_p\varphi_2 = \frac{1}{\sqrt{2}}([(c\bar{s})^0(s\bar{c})^1]^1 + [(c\bar{s})^1(s\bar{c})^0]^1), \quad (24)$$

$$\chi_p\varphi_3 = \frac{1}{\sqrt{2}}([(cs)^0(\bar{c}\,\bar{s})^1]^1 + [(cs)^1(\bar{c}\,\bar{s})^0]^1), \quad (25)$$

$$\chi_1\varphi_1 = [(c\bar{c})^0(s\bar{s})^0]^0, \qquad \chi_2\varphi_1 = [(c\bar{c})^1(s\bar{s})^1]^0, \quad (26)$$

$$\chi_1\varphi_2 = [(c\bar{s})^0(s\bar{c})^0]^0, \qquad \chi_2\varphi_2 = [(c\bar{s})^1(s\bar{c})^1]^0, \quad (27)$$

$$\chi_1\varphi_3 = [(cs)^0(\bar{c}\,\bar{s})^0]^0, \qquad \chi_2\varphi_3 = [(cs)^1(\bar{c}\,\bar{s})^1]^0, \quad (28)$$

$$\chi_6\varphi_1 = [(c\bar{c})^1(s\bar{s})^1]^2 \quad (29)$$

TABLE III. Energy of S-wave $cs\bar{c}\,\bar{s}$ tetraquark states with $J^{PC} = 1^{++}$ (in mega-electron-volts).

Channel	E_{1S}	E_{c1}	E'_{c1}	$E^{\rm theo}_{\rm th}$	$E^{\rm exp}_{\rm th}$
$\psi_S\chi_5\varphi_1\omega_1$	4112.7	4112.7	4116.9	4112.2	4116.4 ($J/\psi\phi$)
$\psi_S\chi_5\varphi_1\omega_2$	4305.2	4305.2	4309.4		
$\psi_S\chi_p\varphi_2\omega_1$	4033.8	4033.7	4080.7	4033.5	4080.5 ($D_sD_s^*$)
$\psi_S\chi_p\varphi_2\omega_2$	4370.6	4370.8	4417.8		
$\psi_S\chi_p\varphi_3\omega_3$	4343.4	4332.7	...		
$\psi_S\chi_p\varphi_3\omega_4$	4361.5	4374.3	...		

$$\chi_6\varphi_2 = [(c\bar{s})^1(s\bar{c})^1]^2 \quad (30)$$

$$\chi_6\varphi_3 = [(cs)^1(\bar{c}\,\bar{s})^1]^2, \quad (31)$$

where the χ_p in Eqs. (24) and (25) is $\frac{1}{\sqrt{2}}(\chi_3 + \chi_4)$.

Generally, we only consider the S-wave states for the low-lying state, i.e., $L_r = 0$ for states with $J^{PC} = 1^{++}$. However, for the high-lying states, $X(4500)$ and $X(4700)$, we will take into account the D-wave states, i.e., $L_r = 2$ for some states with $J^{PC} = 0^{++}$.

First, we calculated the energies of the S-wave $cs\bar{c}\,\bar{s}$ states with $J^{PC} = 1^{++}$ and 0^{++}. The results are given in Tables III and IV, respectively. In the tables, E_{1S} (E_{2S}) denotes the energy of the first (second) S-wave state with single channel calculation, and $E_{c1}(E_{c2})$ represents the energy through coupling of two different color structures. $E^{\rm theo}_{\rm th}(E^{\rm exp}_{\rm th})$ represents the theoretical (experimental) two-body threshold. Because the theoretical calculation cannot reproduce the experimental data exactly for the meson spectrum, we make a correction, $E' = E - E^{\rm theo}_{\rm th} + E^{\rm exp}_{\rm th}$, for the meson-meson configuration to minimize the theoretical uncertainty. $E'_{c1}(E'_{c2})$ represents the corrected energy of $E_{c1}(E_{c2})$. For the diquark-antidiquark configuration, the correction is not applied because of no asymptotic physical state in this case.

From Tables III and IV, we can see that the energies of the color singlet-singlet $(1 \otimes 1)$ structure are all a bit higher than the corresponding theoretical thresholds. The adiabatic energy of the system in this case is shown in Fig. 1 (the adiabatic energy is obtained by setting the number of Gaussians for the relative motion between two subclusters to 1). When we gradually increase the distance between the two subclusters, the energy slowly tends to the theoretical threshold. This phenomenon suggests that the two mesons tend to stay away and no bound states can be formed when the color structure is $1 \otimes 1$. The reason for this phenomenon is that the Goldstone bosons exchange between the two subclusters is too weak to bind the two mesons together. When the color structure is octet-octet $(8 \otimes 8)$, the energies are generally higher than the corresponding color singlet-singlet $(1 \otimes 1)$ structure. According to Fig. 1(b), the two colorful subclusters cannot fall apart or

TABLE IV. Energy of S-wave $cs\bar{c}\,\bar{s}$ tetraquark states with $J^{PC}=0^{++}$ (in mega-electron-volts).

Channel	E_{1S}	E_{c1}	E'_{c1}	$E_{\rm th}^{\rm theo}$	$E_{\rm th}^{\rm exp}$	E_{2S}	E_{c2}	E'_{c2}
$\psi_S\chi_1\varphi_1\omega_1$	3810.7	3810.6	3942.0	3810.3	3941.7 ($\eta_c\eta'$)			
$\psi_S\chi_1\varphi_1\omega_2$	4359.1	4360.2	4491.6			4712.7		4844.1
$\psi_S\chi_2\varphi_1\omega_1$	4114.0	4114.0	4118.2	4112.2	4116.4 ($J/\psi\phi$)			
$\psi_S\chi_2\varphi_1\omega_2$	4273.4	4273.4	4277.6			4601.2		4605.4
$\psi_S\chi_1\varphi_2\omega_1$	3908.0	3908.0	3837.8	3906.8	3936.6 (D_sD_s)			
$\psi_S\chi_1\varphi_2\omega_2$	4376.1	4376.3	4406.1			4910.6		4940.4
$\psi_S\chi_2\varphi_2\omega_1$	4161.6	4161.6	4225.6	4160.4	4224.4 ($D_s^*D_s^*$)			
$\psi_S\chi_2\varphi_2\omega_2$	4304.8	4304.4	4368.4			4655.4		4719.4
$\psi_S\chi_1\varphi_3\omega_3$	4323.7	4319.1	$\cdots$			4643.5	4641.7	$\cdots$
$\psi_S\chi_1\varphi_3\omega_4$	4384.9	4390.0	$\cdots$			4976.5	4980.4	$\cdots$
$\psi_S\chi_2\varphi_3\omega_3$	4370.0	4376.1	$\cdots$			4924.3	4926.8	$\cdots$
$\psi_S\chi_2\varphi_3\omega_4$	4304.2	4292.1	$\cdots$			4607.4	4601.4	$\cdots$

get too close. That is because the existence of confinement V_C prevents the far separation of the two colorful clusters. This phenomenon suggests that the resonances with compact tetraquark structure may exist in our present calculation when the color configuration of the meson-meson configuration is octet-octet $(8\otimes 8)$. Because of the small overlap between the two color structures, $1\otimes 1$ and $8\otimes 8$, the coupling between two color structures is small, which makes the resonance possible. When the configuration is diquark-antidiquark, the two color structures antitriplet-triplet $(\bar{3}\otimes 3)$ and sextet-antisextet $(6\otimes\bar{6})$ have similar energies, and the coupling between them is rather strong. According to Figs. 1(c) and 1(d), whether $\bar{3}\otimes 3$ or $6\otimes\bar{6}$, the two subclusters are both colorful, and they cannot stay too far away from each other, and short-range repulsion prevents the two subclusters from getting too close. So, the resonances with compact tetraquark structure may also exist in the diquark-antidiquark configuration.

For the states with $J^{PC}=1^{++}$ (Table III), the energies of the $1S$ ground state are all between 4300 and 4420 MeV except the state with color structure $1\otimes 1$. The corrected energy E'_{c1} of the hidden color $(8\otimes 8)$ channel is around 4309.4 MeV, and the lowest energy of the diquark-antidiquark configuration is about 4332 MeV. Both energies are not far from the mass of $X(4274)$. The mix of two configurations may reduce the energy a little, and the lowest energy of the state with $J^{PC}=1^{++}$ is expected to approach the experimental value of the $X(4274)$. So, the $X(4274)$ can be a candidate of the compact tetraquark state in our present calculation. As for $X(4140)$, the energy is too low, and there is no matching state for it in our calculations, which is different from the results of Refs. [10,13,16,17]. For the states with $J^{PC}=0^{++}$ (Table IV), the energies of $1S$ ground state are all between 4277 and 4492 MeV except the state with color structure $1\otimes 1$. It is worth mentioning that the energy of the $X(4350)$, which was reported by Belle Collaboration in the $\gamma\gamma\to J/\psi\phi$ process, is close to the energy of hidden color $(8\otimes 8)$ state of $(c\bar{s})(s\bar{c})$, 4368.4 MeV. If the J^{PC} of $X(4350)$ can be determined to be 0^{++}, we think it can be a candidate for the compact tetraquark state, which agrees with the results of the Born-Oppenheimer approach, in which a mass of 4370 MeV was obtained [17]. As for the $2S$ radial excitation, the energy of a hidden color $(8\otimes 8)$ state of $(c\bar{s})(s\bar{c})$ is 4719.4 MeV, which is very close to the mass of the $X(4700)$ found by the LHCb Collaboration. In addition to the hidden-color state with color structure $8\otimes 8$, the $2S$ states with the diquark-antidiquark configuration have energies around 4650 MeV, which are not much different from the $X(4700)$, too. So, the $X(4700)$ can be explained to be a $2S$ radial excited state with a compact tetraquark structure in our calculation, which agrees with the results of diquark model and color flux-tube model [11,12]. The other exotic resonance recently found in the experiment by the LHCb Collaboration is $X(4500)$, but there is no matching state for it in our calculations. Whether $X(4500)$ can be explained by the tetraquark structure requires further study.

For the D-wave states with $J^{PC}=0^{++}$ (see Table V), the energies of the meson-meson configuration with color structure $1\otimes 1$ are still very close to the corresponding theoretical threshold. That is because the too-far distance between the two clusters makes the effect of the D-wave excitation negligible. When the color structure is $8\otimes 8$ or the configuration is diquark-antidiquark, the energies of D-wave excitation are all too high to be explained as the $X(4700)$ and $X(4500)$. So it is not appropriate to use angular excitation to explain these exotic resonances in our present calculation.

To analyze the spacial structure of the $cs\bar{c}\,\bar{s}$ tetraquark, we calculated the distances between two $q(\bar{q})$ for $(c\bar{s})(s\bar{c})$ and $(cs)(\bar{c}\,\bar{s})$ ground states with $J^{PC}=0^{++}$ (see Tables VI and VII). According to Table VI, when the color structure is $1\otimes 1$, the distance between the two $q(\bar{q})$, which are in two different subclusters, is big. This phenomenon shows that two subclusters tend to stay away from each other. When the color structure is $8\otimes 8$, the distances between any two $q(\bar{q})$ are all very close, and now the structure is a compact tetraquark structure. After coupling the two color structures

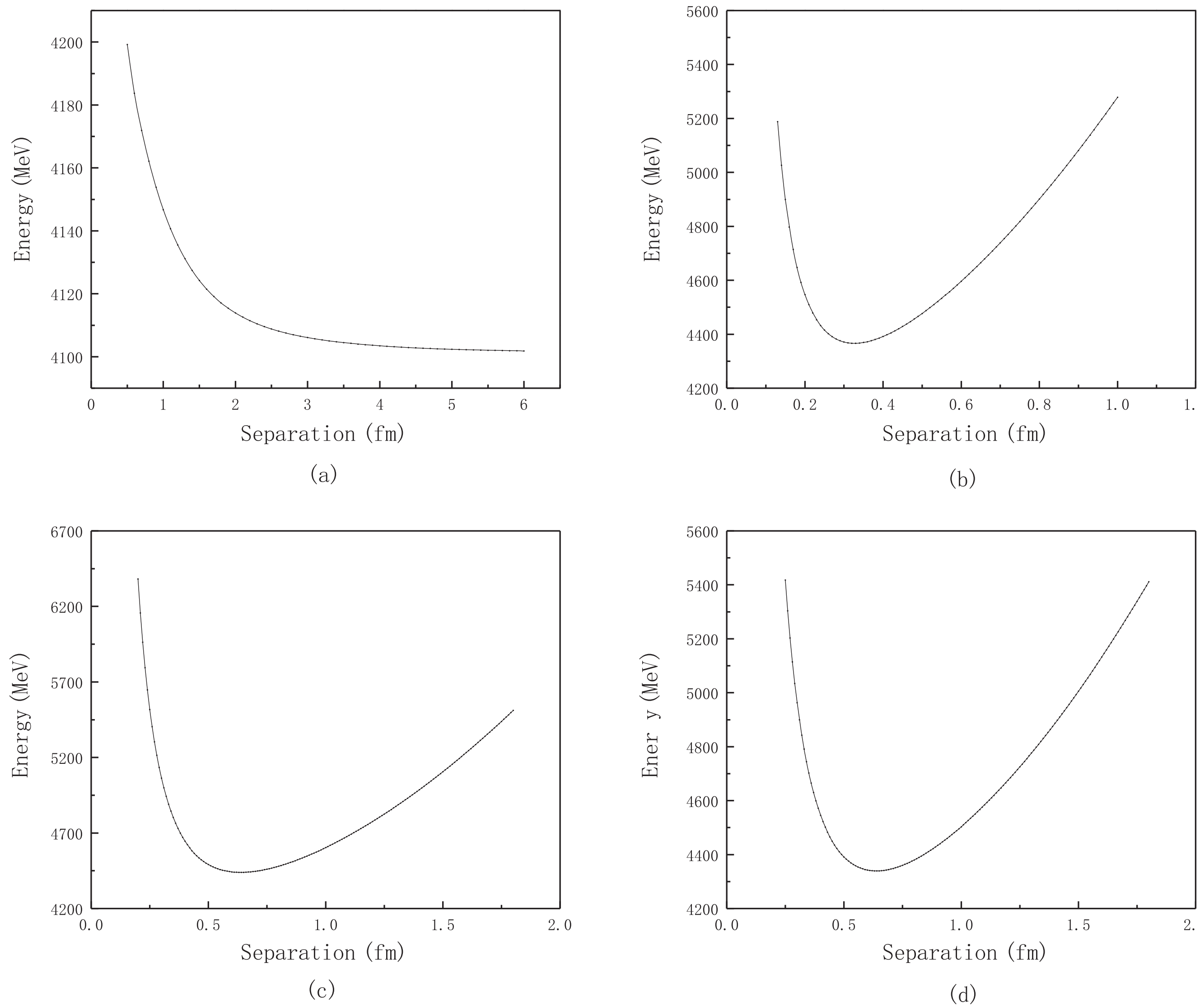

FIG. 1. Energy of $cs\bar{c}\,\bar{s}$ tetraquark states with different color structures as a function of the distance between two subclusters. (a) $1\otimes 1$, (b) $8\otimes 8$, (c) $\bar{3}\otimes 3$, and (d) $6\otimes\bar{6}$.

for the meson-meson configuration, the change is small because of the weak coupling between these two color structures. For the diquark-antiquark configuration in Table VII, the distance between any two $q(\bar{q})$ is small, and now the structure is also very compact. After coupling the two color structures for the diquark-antiquark configuration, the change is obvious. Strong coupling between these two color structures is the cause of this phenomenon.

TABLE V. Energy of D-wave $cs\bar{c}\,\bar{s}$ tetraquark states with $J^{PC}=0^{++}$.(in mega-electron-volts).

Channel	E_{1D}	E_{c1}	E'_{c1}	$E_{\rm th}^{\rm theo}$	$E_{\rm th}^{\rm exp}$
$[\psi_D\chi_6]^0\varphi_1\omega_1$	4116.6	4116.4	4120.6	4112.2	4116.4 $(J/\psi\phi)$
$[\psi_D\chi_6]^0\varphi_1\omega_2$	5173.8	5174.0	5178.2		
$[\psi_D\chi_6]^0\varphi_2\omega_1$	4163.5	4163.2	4227.2	4160.4	4224.4 $(D_s^*D_s^*)$
$[\psi_D\chi_6]^0\varphi_2\omega_2$	5141.0	5141.0	5205.0		
$[\psi_D\chi_6]^0\varphi_3\omega_3$	4853.8	4847.6	⋯		
$[\psi_D\chi_6]^0\varphi_3\omega_4$	5173.8	5177.6	⋯		

TABLE VI. Distance between $q(\bar{q})$ and $q(\bar{q})$ for $(c\bar{s})(s\bar{c})$ ground states with $J^{PC}=0^{++}$.

Channel	$c\bar{s}$	$s\bar{c}$	cs	$\bar{s}\,\bar{c}$	$c\bar{c}$	$\bar{s}s$
$\psi_S\chi_1\varphi_2\omega_1$	0.50	0.50	5.86	5.86	5.84	5.87
$\psi_S\chi_1\varphi_2\omega_2$	0.70	0.70	0.67	0.67	0.44	0.84
Coupling	0.50	0.50	5.86	5.86	5.84	5.87
	0.71	0.71	0.68	0.68	0.43	0.85
$\psi_S\chi_2\varphi_1\omega_1$	0.60	0.60	5.86	5.86	5.85	5.88
$\psi_S\chi_2\varphi_1\omega_2$	0.67	0.67	0.64	0.64	0.42	0.80
Coupling	0.60	0.60	5.86	5.86	5.85	5.88
	0.69	0.69	0.68	0.68	0.46	0.85

TABLE VII. Distance between $q(\bar{q})$ and $q(\bar{q})$ for $(cs)(\bar{c}\bar{s})$ ground states with $J^{PC} = 0^{++}$.

Channel	cs	$\bar{c}\bar{s}$	$c\bar{c}$	$s\bar{s}$	$c\bar{s}$	$s\bar{c}$
$\psi_S\chi_1\varphi_3\omega_3$	0.61	0.61	0.51	0.80	0.67	0.67
$\psi_S\chi_1\varphi_3\omega_4$	0.71	0.71	0.44	0.85	0.68	0.68
Coupling	0.59	0.59	0.32	0.69	0.54	0.54
	0.75	0.75	0.57	0.96	0.79	0.79
$\psi_S\chi_2\varphi_3\omega_3$	0.63	0.63	0.50	0.82	0.68	0.68
$\psi_S\chi_2\varphi_3\omega_4$	0.67	0.67	0.41	0.80	0.63	0.63
Coupling	0.42	0.42	0.37	0.56	0.48	0.48
	0.83	0.83	0.52	0.99	0.79	0.79

In addition, the relative kinetic energy between two light $q(\bar{q})$ is greater than that of two heavy $q(\bar{q})$. That is why the distance between two light $q(\bar{q})$ is bigger than that of two heavy $q(\bar{q})$ in our calculations.

IV. CONCLUSIONS

In this work, we investigated the $cs\bar{c}\bar{s}$ tetraquark states in the framework of chiral quark model and tried to explain those exotic resonances recently observed in the invariant mass distribution of $J/\psi\phi$. Two configurations, $(q\bar{q})(q\bar{q})$ and $(qq)(\bar{q}\bar{q})$, with all possible spin and color structures were taken into consideration. We found that the $(q\bar{q})(q\bar{q})$ configuration cannot form the bound states when the color structure is $1\otimes 1$ because the Goldstone bosons exchange is too weak to bound the two mesons. If the color structure of $(q\bar{q})(q\bar{q})$ is $8\otimes 8$ or the configuration is $(qq)(\bar{q}\bar{q})$, the resonances can be formed. In our calculation, the $X(4274)$ and $X(4350)$ in experiment can be regarded as the ground state of $cs\bar{c}\bar{s}$ compact tetraquark states. The $X(4700)$ can be explained to be the $2S$ radial excitation, but the $X(4500)$ has no match in the present calculation. Because of the too-low energy of $X(4140)$, it is impossible to use the tetraquark state to explain this exotic resonances in our work. The current work does not consider the coupling between the configurations $(q\bar{q})(q\bar{q})$ and $(qq)(\bar{q}\bar{q})$, and the coupling of the S wave and D wave is also ignored. These legacy situations will be considered in future work.

ACKNOWLEDGMENTS

This work is supported partly by the National Natural Science Foundation of China under Contracts No. 11675080, No. 11775118, No. 11847145, and No. 11535005.

[1] T. Aaltonen *et al.* (CDF Collaboration), Phys. Rev. Lett. **102**, 242002 (2009).
[2] C. P. Shen *et al.* (Belle Collaboration), Phys. Rev. Lett. **104**, 112004 (2010).
[3] R. Aaij *et al.* (LHCb Collaboration), Phys. Rev. D **85**, 091103 (2012).
[4] V. M. Abazov *et al.* (D0 Collaboration), Phys. Rev. D **89**, 012004 (2014).
[5] S. Chatrchyan *et al.* (CMS Collaboration), Phys. Lett. B **734**, 261 (2014).
[6] J. P. Lees *et al.* (*BABAR* Collaboration), Phys. Rev. D **91**, 012003 (2015).
[7] T. Aaltonen *et al.* (CDF Collaboration), Mod. Phys. Lett. A **32**, 1750139 (2017).
[8] R. Aaij *et al.* (LHCb Collaboration), Phys. Rev. Lett. **118**, 022003 (2017).
[9] R. Aaij *et al.* (LHCb Collaboration), Phys. Rev. D **95**, 012002 (2017).
[10] Qi-Fang Lü and Yu-Bing Dong, Phys. Rev. D **94**, 074007 (2016).
[11] J. Wu, Y. R. Liu, K. Chen, X. Liu, and S. L. Zhu, Phys. Rev. D **94**, 094031 (2016).
[12] C. R. Deng, J. L. Ping, H. X. Huang, and F. Wang, Phys. Rev. D **98**, 014026 (2018).
[13] Fl Stancu, J. Phys. G **37**, 075017 (2010).
[14] P. G. Ortega, J. Segovia, D. R. Entem, and F. Fernández, Phys. Rev. D **94**, 114018 (2016).
[15] H. X. Chen, E. L. Cui, W. Chen, X. Liu, and S. L. Zhu, Eur. Phys. J. C **77**, 160 (2017).
[16] R. F. Lebed and A. D. Polosa, Phys. Rev. D **93**, 094024 (2016).
[17] E. Braaten, C. Langmack, and D. H. Smith, Phys. Rev. D **90**, 014044 (2014).
[18] L. Maiani, A. D. Polosa, and V. Riquer, arXiv:1903.10253.
[19] J. Vijande, F. Fernández, and A. Valcarce, J. Phys. G **31**, 481 (2005).
[20] A. Valcarce, H. Garcilazo, F. Fernández, and P. González, Rep. Prog. Phys. **68**, 965 (2005).
[21] E. Hiyama, Y. Kino, and M. Kamimura, Prog. Part. Nucl. Phys. **51**, 223 (2003).
[22] C. R. Deng, J. L. Ping, H. X. Huang, and F. Wang, Phys. Rev. D **92**, 034027 (2015).
[23] H. X. Huang, J. L. Ping, and F. Wang, Phys. Rev. C **89**, 034001 (2014).
[24] X. Y. Chen and J. L. Ping, Phys. Rev. D **98**, 054022 (2018).
[25] M. Tanabashi *et al.* (Particle Data Group), Phys. Rev. D **98**, 030001 (2018).
[26] L. Maiani, A. D. Polosa, and V. Riquer, Phys. Rev. D **94**, 054026 (2016).